Electronic Supporting Information

Minimization of Ion Transport Resistance: Diblock Copolymer Micelles Derived Hierarchical Pores Arm Nitrogen-Doped Carbon Spheres for Superior Rate and Power Zn-Ion Capacitors

Jun Huang,[a] Li Wang,[a] Zhongyou Peng,[a] Mengke Peng,[a] Longbin Li,[a] Xiannong Tang,[a] Yazhou Xu,[a] Licheng Tan,[a] Kai Yuan,[a]* and Yiwang Chen[a,b]*

[a] College of Chemistry/Institute of Polymers and Energy Chemistry, Nanchang University, 999 Xuefu Avenue, Nanchang 330031, China.
[b] Institute of Advanced Scientific Research (iASR), Jiangxi Normal University, 99 Ziyang Avenue, Nanchang 330022, China.

Corresponding Author

*Dr. Kai Yuan E-mail: kai.yuan@ncu.edu.cn.

* Dr. Yiwang Chen E-mail: ywchen@ncu.edu.cn.

Experimental Section

Chemicals. Dopamine hydrochloride (DA) was purchased from Sigma Aldrich. Amphiphilic block copolymer, polystyrene-*b*-poly(ethylene oxide) (PS_{62}-*b*-PEO_{119}) was purchased from Xi'an Ruixi Biological Technology Co., Ltd. All of chemicals were of analytical grade and used without further purification.

Synthesis of nitrogen-doped hierarchically porous carbon spheres (N-HPCSs). The N-HPCSs were synthesized by controlled polymerization of DA and PS_{62}-*b*-PEO_{119}. First, 200 mg of DA was dissolved in the mixed solution (12 mL) of ethanol and deionized water (with volume ratio of 1:2). Then, the above solution poured into 4 mL of THF containing 30 mg of PS_{62}-*b*-PEO_{119} under mild stirring at room temperature. After 1 hour, 0.5 mL of ammonia aqueous solution (NH_4OH, 28-30%) was injected to induce the self-polymerization of DA and the colour of the solution became brown. After continuous reaction for 20 hours at room temperature, PDA/PS_{62}-*b*-PEO_{119} composite spheres were obtained by centrifugation and washed with mixed solution of ethanol and deionized water for several times. For carbonization, the PDA/PS_{62}-*b*-PEO_{119} composite spheres were pre-heated at 350 ^oC for 3 hours and finally heated at 800 ^oC for 2 hours under nitrogen atmospheres with a heating rate of 1 $^oC\ min^{-1}$. Finally, N-HPCSs with the average particle size of *ca.* 250 nm were obtained. The N-doped carbon spheres (N-CSs) were prepared by the same method with N-HPCSs except for the absence of PS_{62}-*b*-PEO_{119}.

Materials Characterization. The morphology and structure features of the samples were investigated by a field-emission scanning microscope (JEOL JSM-6700F, 15 keV), and a field-emission transmission electron microscope (JEOL JEM-2100F, 200 keV). HAADF-STEM characterization was performed on a field emission transition electron microscope (JEM-ARM200F, 200 kV) equipped with double spherical aberration correctors for the condenser lens and objective lens. The crystalline structure was studied on a Bruker D8-A25 diffractometer with Cu Kα radiation (λ = 1.5406 Å). The elemental composition and chemical state of the samples were investgated by XPS (Kratos Axis Ultra Dld). The surface characteristics of the samples were studied by gas physisorption at 77 K on an automated apparatus (Micromeritics, ASAP 2010). Thermogravimetric (TG) analysis measurements were carried out using a SDT Q600 instrument in a temperature range of room temperature to 1000 °C at a heating rate of 10 °C min^{-1} under N_2 flow. The surface area of the samples were obtained by N_2 adsorption/desorption isotherms at 77 K that were conducted on a Quantachrome Autosorb-iQ instrument. In addition, to conduct *ex situ* tests including SEM, TEM, XRD, and XPS, the cathodes were charged/discharged to specifc potentials, washed with distilled water to get rid of electrolyte residual and dried overnight in a vacuum oven before test.

Electrochemical Measurements. The electrochemical performance was tested in coin-type cells, which comprised the N-CS and N-HPCS electrode as cathodes, the commercial Zn foil as anode and 2 M $ZnSO_4$ aqueous solution as electrolyte. The

separator was purchased from NKK (Nippon Kodoshi Corporation). N-CS and N-HPCS electrodes were prepared by mixing N-CS and N-HPCS with carbon black (Sigma-Aldrich) and poly(vinylidene fluoride) binder (Sigma-Aldrich) at a weight ratio of 8:1:1 in 1-methyl-2-pyrrolidinone (NMP, Sigma-Aldrich). The mixture was coated on Ti net, and then dried overnight at 60 °C. The total mass loadings of the N-CS and N-HPCS electrodes are 1.0 to 1.2 mg cm^{-2}, while the counter electrode (Zn foil) is 15 mg cm^{-2} with the purpose of excluding the effect of anode fading. The CHI 760E workstation was used to collect cyclic voltammogram, electrochemical impedance spectroscopy, and galvanostatic charge/discharge curves. The long term cycling stability was examined by a CT3001A battery tester (Wuhan LAND electronics Co., Ltd., China). The specific capacity C (mA h g^{-1}), mass energy density E (Wh kg^{-1}) and mass power density P (kW kg^{-1}) was calculated from galvanostatic charge/discharge curves of the devices using the following equations:

$$C = 2I\int Vdt/3.6Vm \quad (1)$$

$$E = I\int Vdt/3.6m \quad (2)$$

$$P = 3600E/t \quad (3)$$

where I (A), t (s), V (V) and m (g) represent the discharge current (A), the discharge time, the voltage window, and the mass of active material in cathode, respectively.

The contribution from diffusion-controlled process and surface reaction of anode and cathode can be evaluated by using CV curves. The relationship between current (I) and scan rate (v) can be written as:

$$I = av^b \quad (4)$$

where a and b are constant can be obtained from log v versus log I plots. When b= 0.5 indicates an ideal diffusion-dominated process and when b = 1.0 indicates surface-determined capacitive-controlled behavior. Furthermore, the capacitive contribution to the total current can be differentiated quantitively by using the following equations:

$$I(V) = k_1 v + k_2 v^{\frac{1}{2}} \quad (5)$$

$$\frac{I(V)}{v^{\frac{1}{2}}} = k_1 v^{\frac{1}{2}} + k_2 \quad (6)$$

where I is the current density at a voltage (V), v is the scan rate (mV/s), k_1 and k_2 can be obtained from the slope and intercept, respectively. Where $k_1 v$ can be attributed to the current from surface capacitance contribution, while $k_2 v^{1/2}$ is indexed to the diffusion process.

The electrochemically active surface area (ECSA) was measured by double layer capacitance (C_{dl}) in a non-Faradaic potential range of 1.3-1.4 V at different scan rates of 2-10 mV s^{-1}. The ECSA was calculated by the following equation:

$$ECSA = C_{dl}/C_{dl(smooth)} \quad (7)$$

where $C_{dl(smooth)}$ is the double layer capacitance value of a smooth surface. The value of $C_{dl(smooth)}$ is 0.04 mF cm^{-2} in this calculation.

The real capacitance ($C'(\omega)$) and imaginary capacitance ($C''(\omega)$) from EIS data were calculated by the following equation:

$$C(\omega) = C'(\omega) + jC''(\omega) \quad (8)$$

where $C'(\omega)$ is the real part of the capacitance $C(\omega)$. $C''(\omega)$ is the imaginary part of the capacitance $C(\omega)$.

The diffusion coefficient of the Zn^{2+} ions can be calculated by Fick's second law:

$$D = R^2T^2/2A^2n^4F^4c^2\sigma^2 \quad (9)$$

where R is the ideal gas constant; T is the applied thermodynamics temperature; F is the Faraday constant; n is the valence; c is the concentration of the Zn^{2+} ions; A is the area of electrode; σ is called the Warburg coefficient.

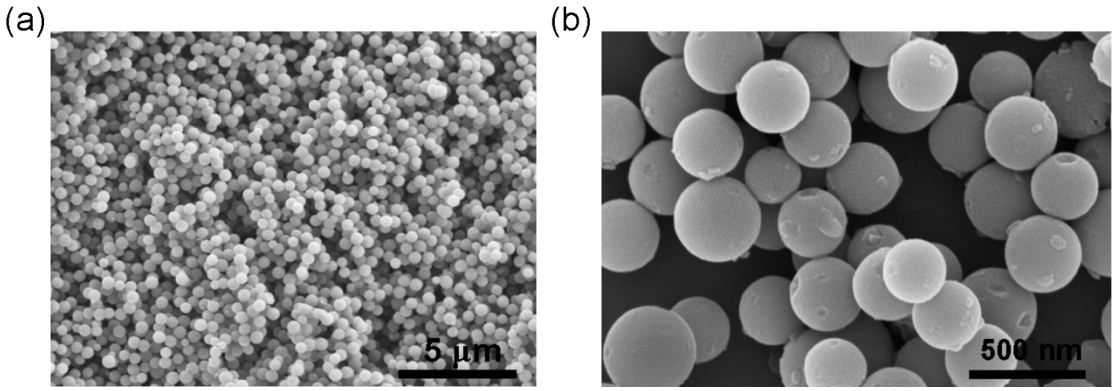

Figure S1. SEM images of N-CS.

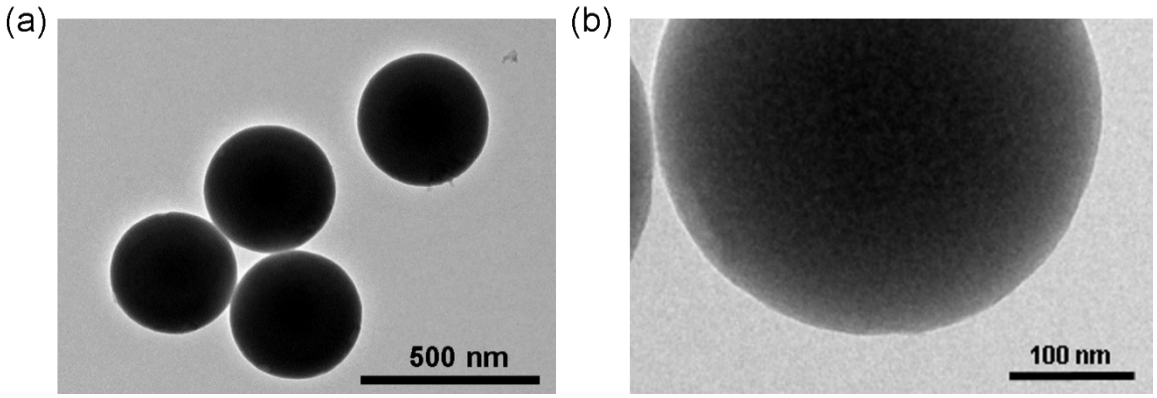

Figure S2. TEM images of N-CS.

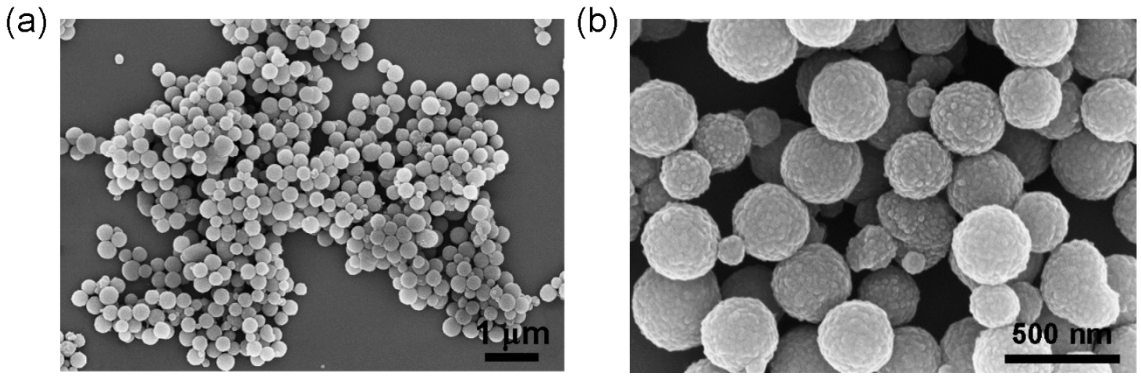

Figure S3. SEM images of PDA/PS-*b*-PEO composite spheres.

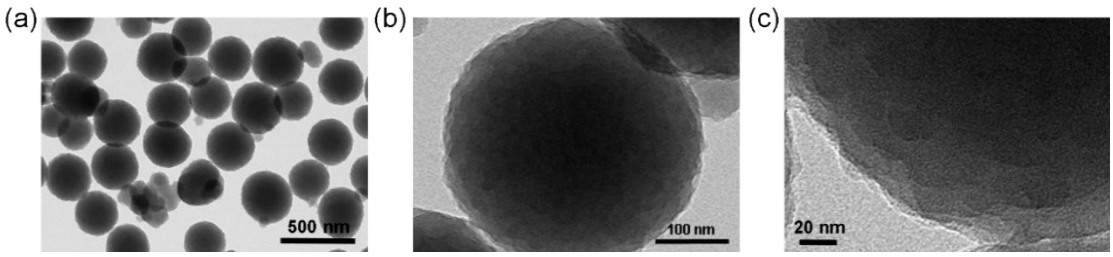

Figure S4. TEM images of PDA/PS-*b*-PEO composite spheres.

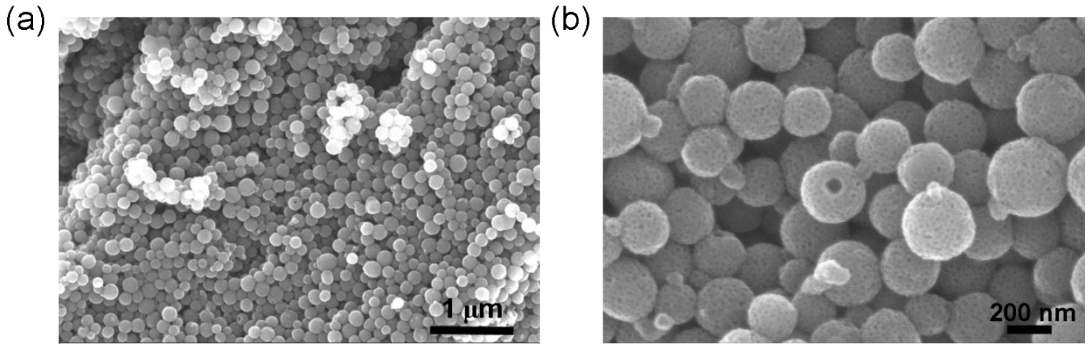

Figure S5. SEM images of N-HPCS.

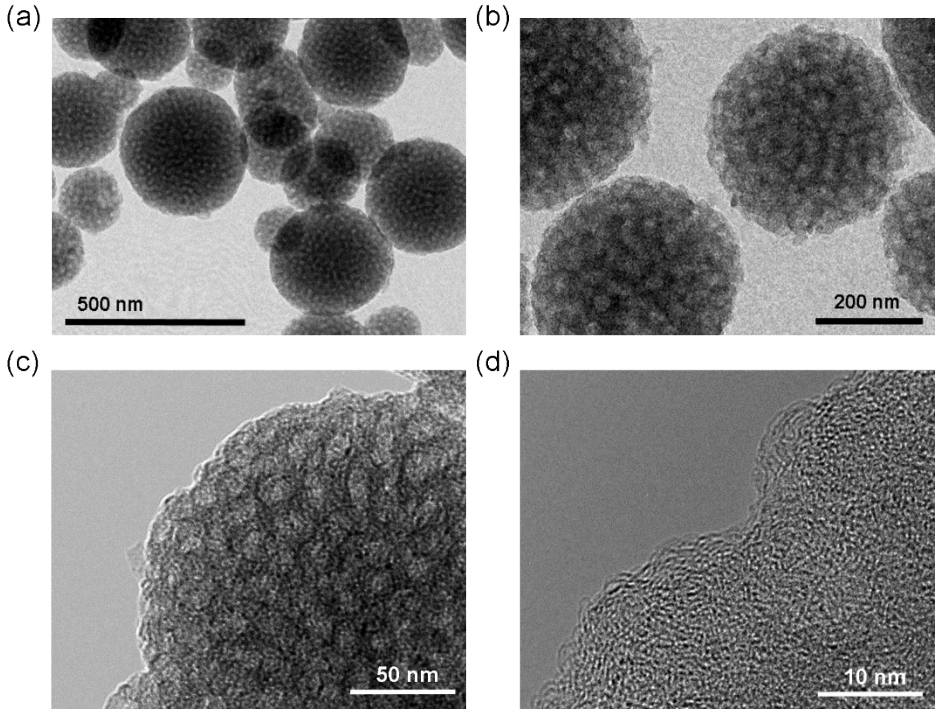

Figure S6. TEM images of N-HPCS.

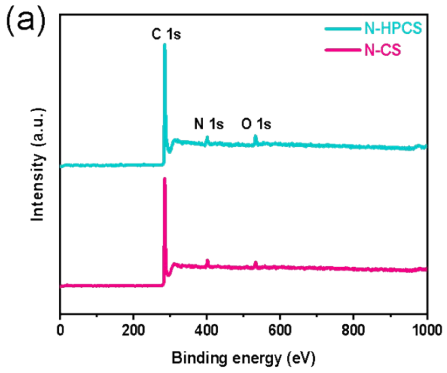

(b)

	N-CS	N-HPCS
C at%	92.84	90.67
N at%	4.05	4.32
O at%	3.11	5.01

Figure S7. (a) XPS spectra and (b) corresponding element contents of N-CS and N-HPCS samples.

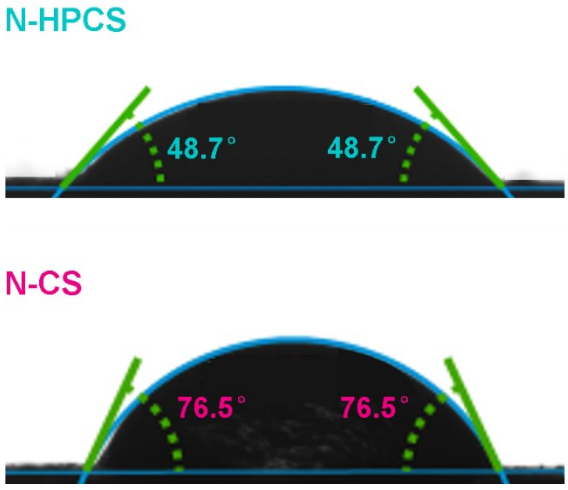

Figure S8. Contact angles of a water droplet on N-CS and N-HPCS samples.

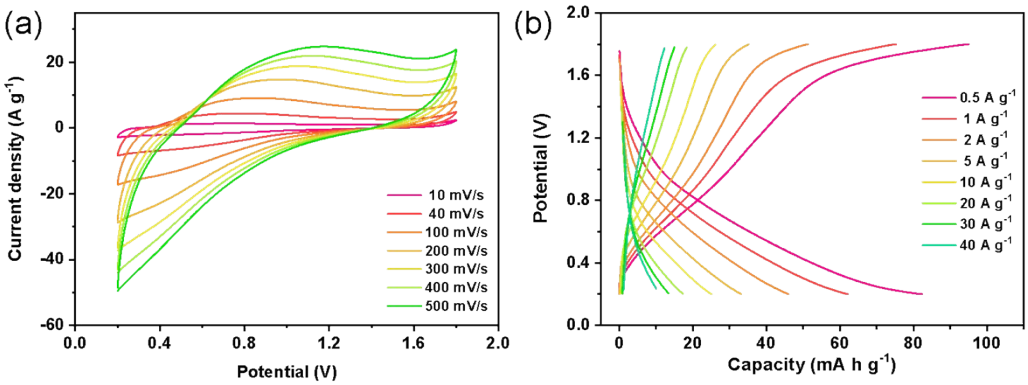

Figure S9. (a) CV and (b) GCD curves of N-CS ZIC.

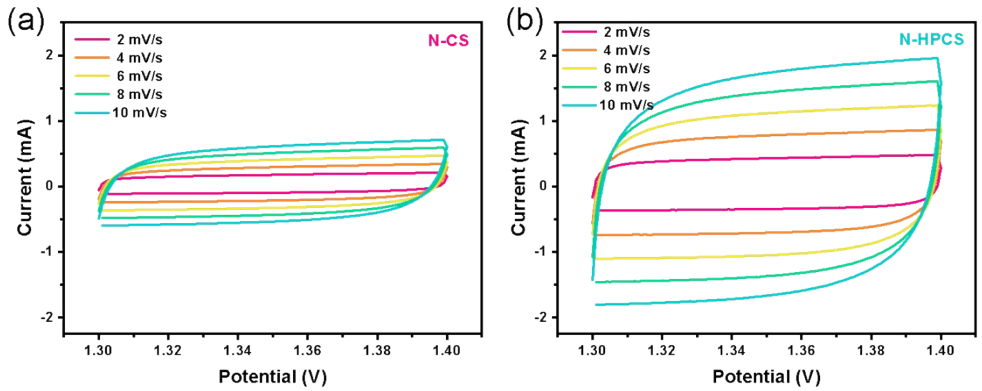

Figure S10. CV curves of (a) N-CS and (b) N-HPCS based ZICs in a non-Faradaic potential range of 1.3-1.4 V at different scan rates.

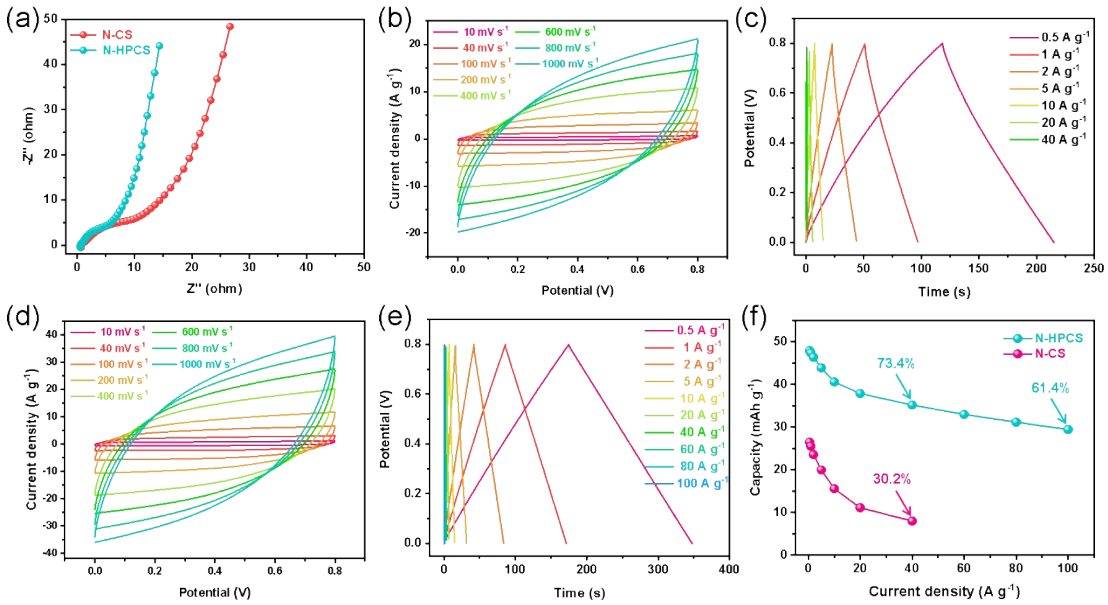

Figure S11. (a) Nyquist plots of N-CS and N-HPCS based symmetric supercapacitors. (b) CV and (c) GCD curves of N-CS supercapacitors. (d) CV and (e) GCD curves of N-MCS supercapacitors. (f) Specific capacities of N-CS and N-HPCS based symmetric supercapacitors at different current densities.

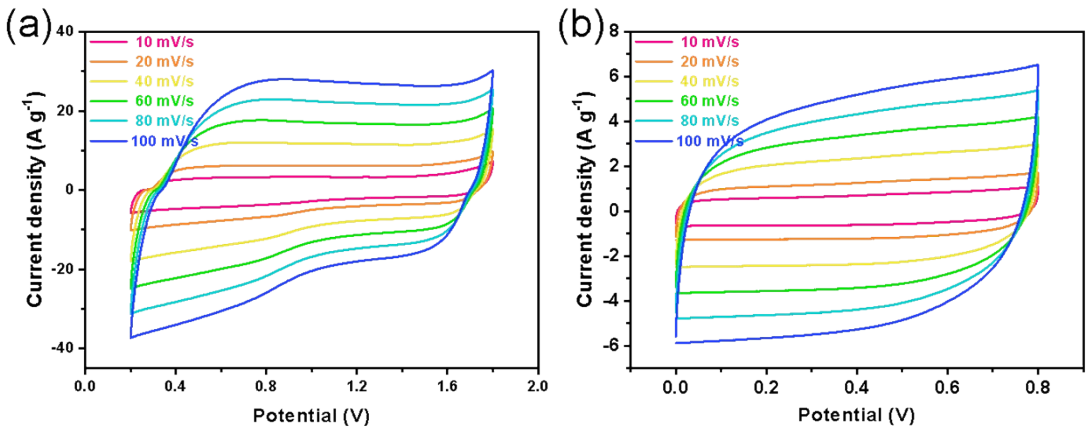

Figure S12. CV curves of (a) N-HPCS ZIC and (b) N-HPCS SC at different scan rates.

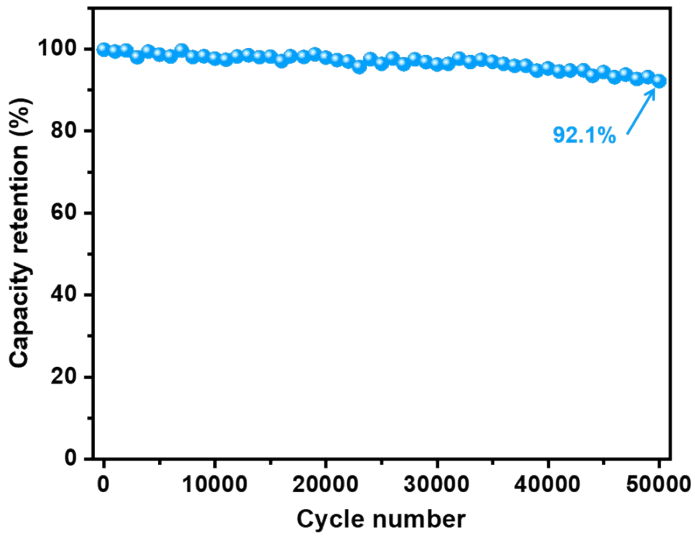

Figure S13. Long-term cycle test of N-CS ZIC at 5 A g^{-1} for 50000 cycles.

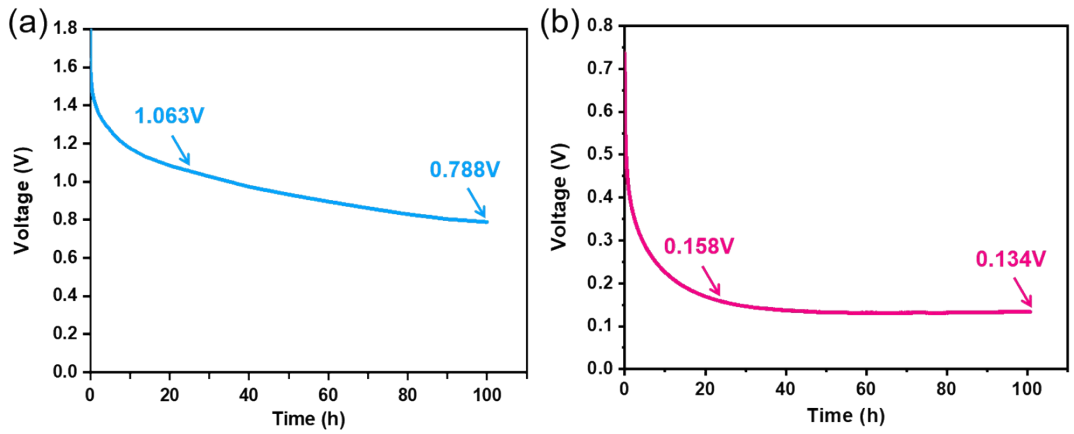

Figure S14. Leakage current curves of (a) N-CS ZIC and (b) N-HPCS SC after self-discharging for 100 h.

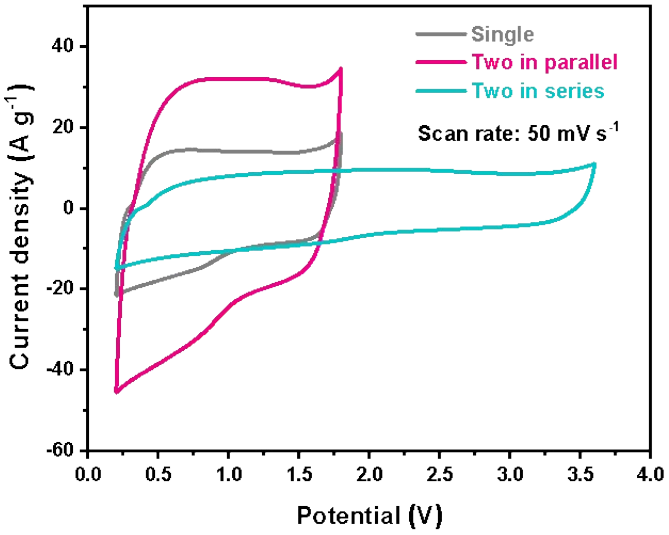

Figure S15. CV curves of single, two-in-series/parallel N-HPCS ZICs at 50 mV s^{-1}.

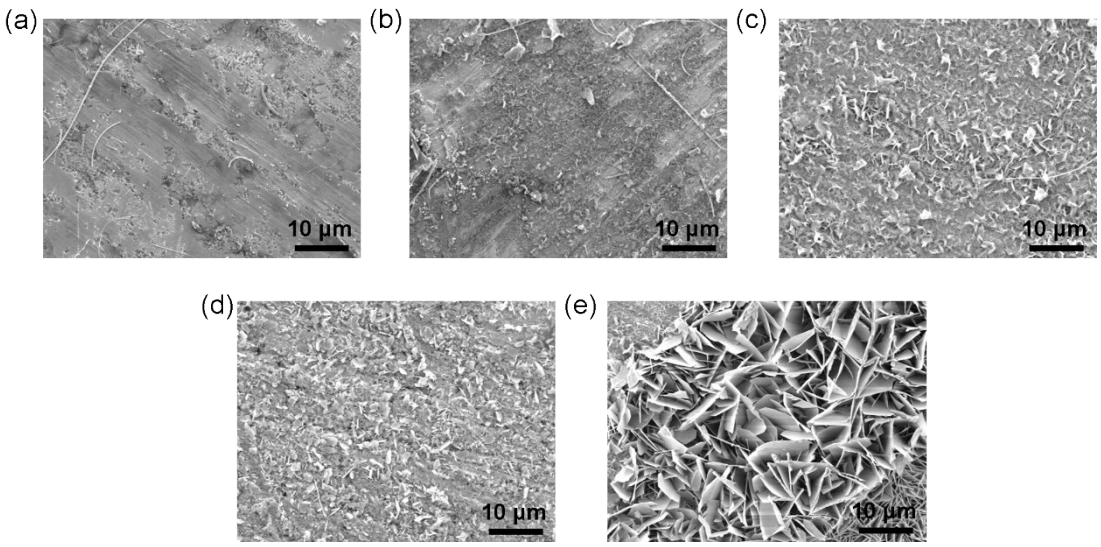

Figure S16. SEM images of Zn foil anode at different discharge-charge states: (a) state A, (b) state B, (c) state C, (d) state D, and (e) state E.

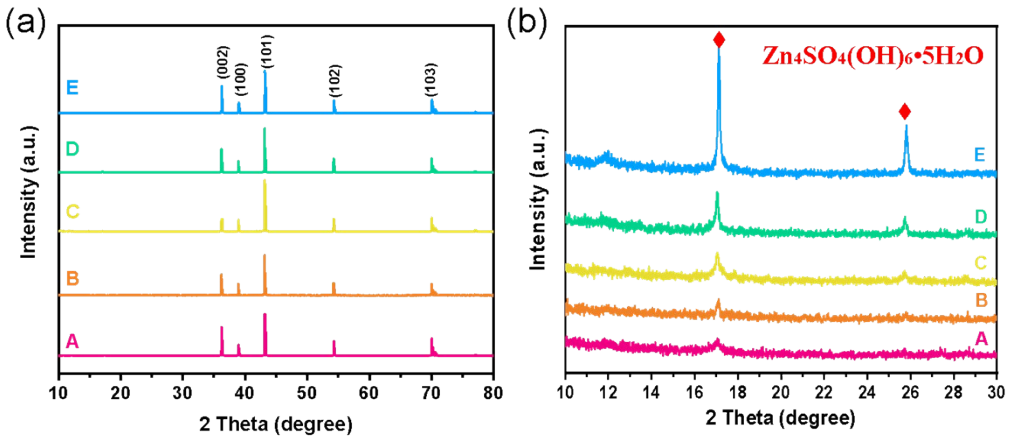

Figure S17. XRD patterns of Zn foil anodes at different discharge-charge states.

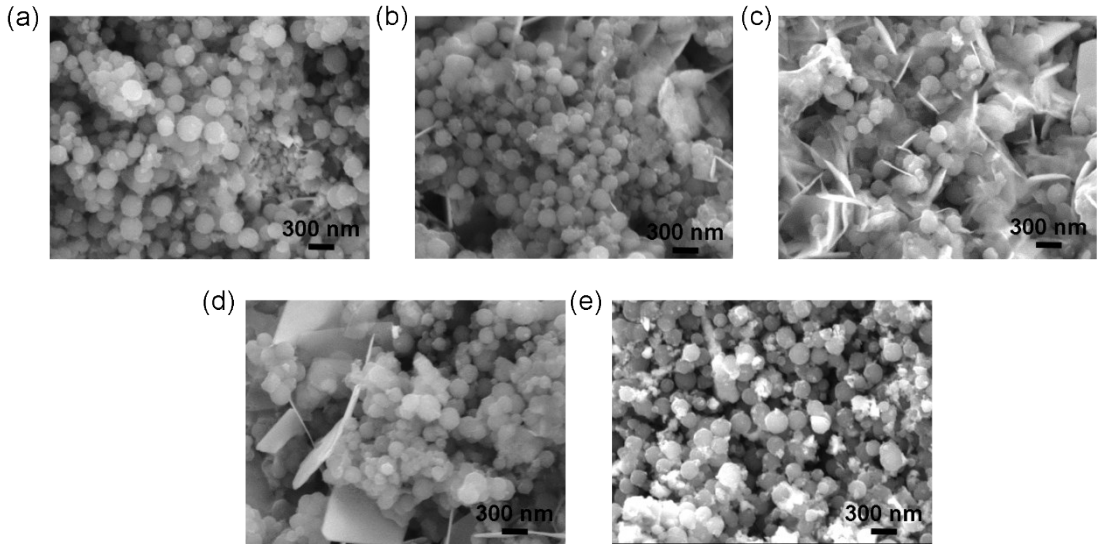

Figure S18. SEM images of N-HPCS cathode at different discharge-charge states: (a) state A, (b) state B, (c) state C, (d) state D, and (e) state E.

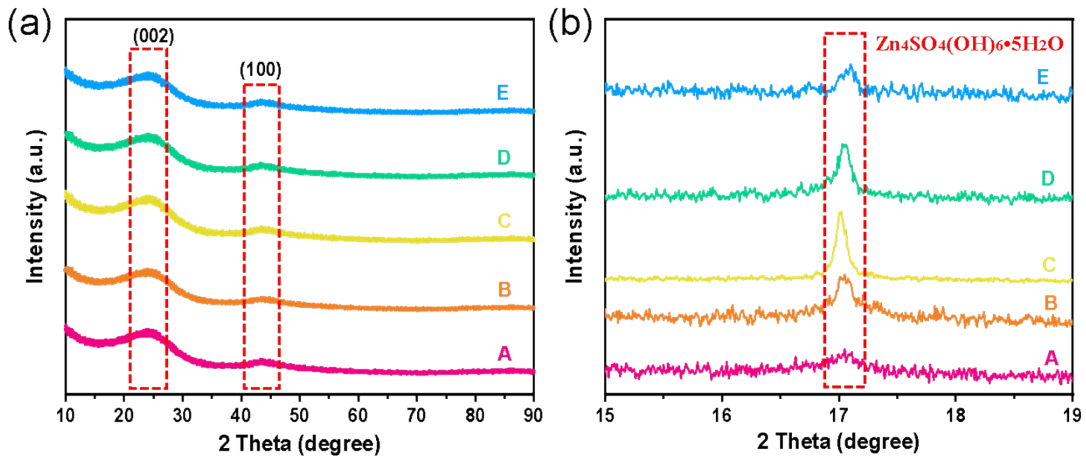

Figure S19. XRD patterns of N-HPCS cathodes at different discharge-charge states.

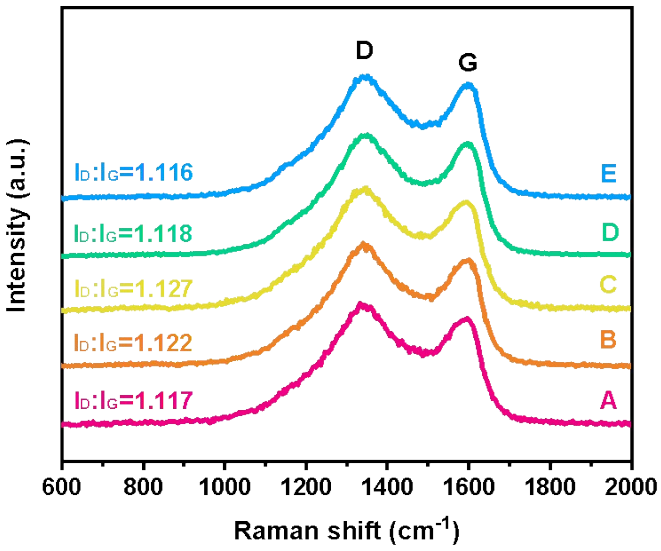

Figure S20. Raman spectra for N-HPCS cathodes at different discharge-charge states.

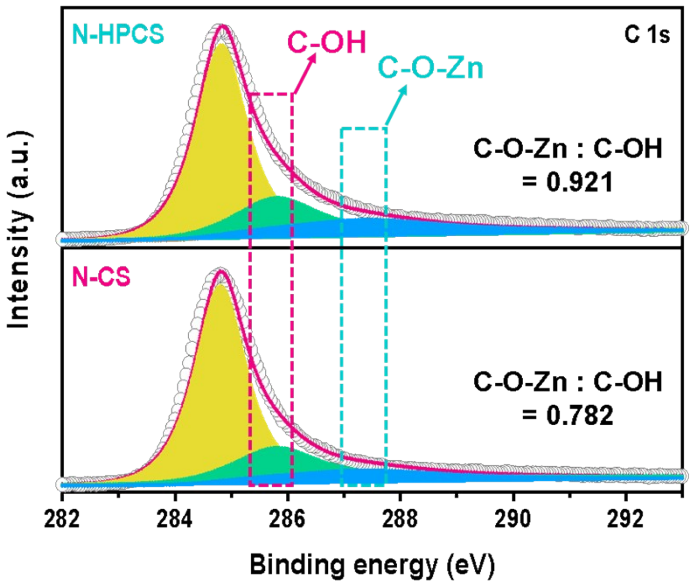

Figure S21. C 1s XPS spectra of N-CS and N-HPCS at 0 V.

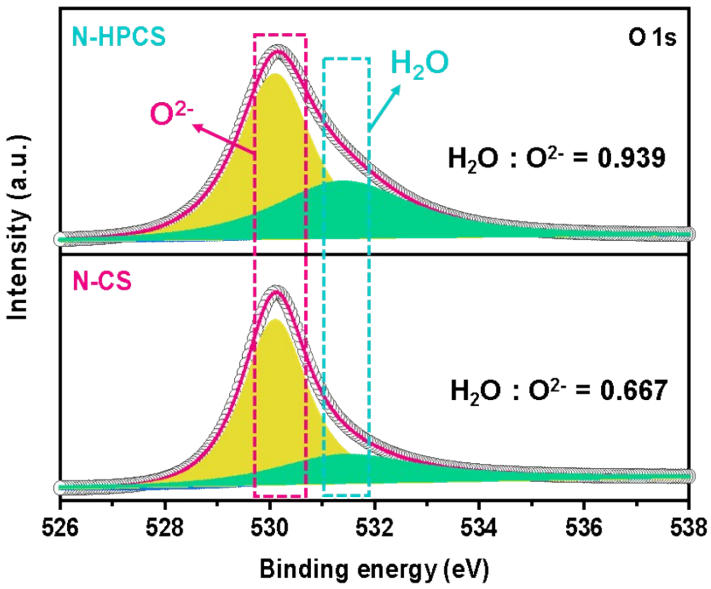

Figure S22. O 1s XPS spectra of N-CS and N-HPCS at 0 V.

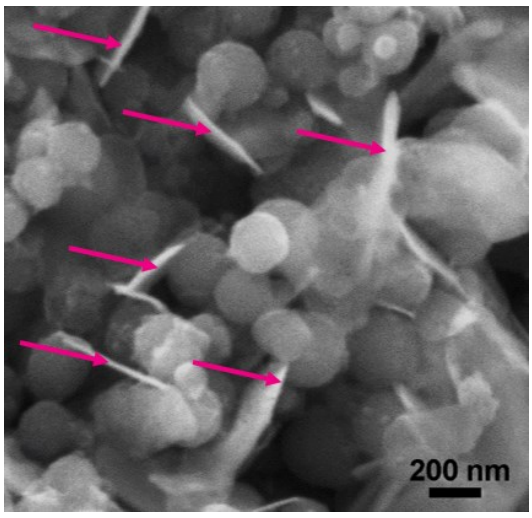

Figure S23. SEM image of the fully discharged N-HPCS electrode. The pink arrows indicate the locations of $Zn_4SO_4(OH)_6 \cdot 5H_2O$ nanosheets.